ACS OMEGA

http://pubs.acs.org/journal/acsodf

Article

Two-Dimensional Porous Structure of V-Doped NiO with Enhanced Electrochromic Properties

Xuhe Zhan,[‖] Feiyu Gao,[‖] Qianyu Zhuang, Yani Zhang, and Jie Dang*

Cite This: *ACS Omega* 2022, 7, 8960−8967

Read Online

ACCESS | Metrics & More | Article Recommendations | Supporting Information

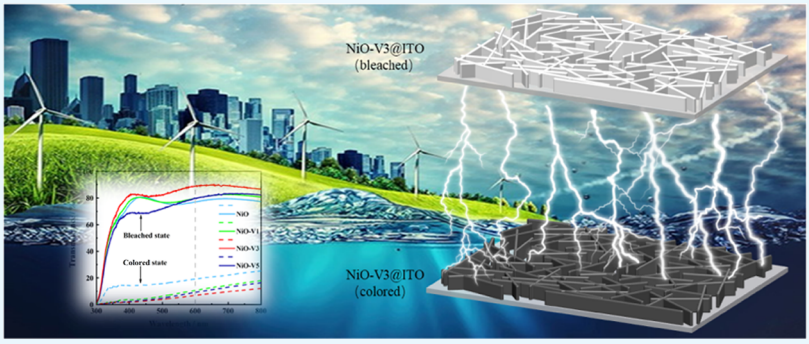

ABSTRACT: In this work, a two-dimensional porous structure of a V-doped NiO film with excellent electrochromic properties on an ITO substrate was synthesized by a hydrothermal method. The influence of V^{5+} ions on the NiO film was explored by adjusting the amount of V doping, including refining the crystal grains, increasing the specific surface area of the film, and accelerating the diffusion rate of OH^- in the film. Compared with the undoped NiO film, a 3 atom % V-doped NiO film comes out with superior electrochromic properties with large optical transmittance modulation (81.9% at 600 nm), fast response times (1.2 and 0.9 s), and excellent cycle stability (90.6%). This work creates innovation direction in the field of intelligent energy-saving window materials with high electrochromic properties.

INTRODUCTION

With the increase in the world's population, environmental pollution and energy shortages have become the greatest challenges facing mankind.[1,2] At present, many researchers around the world are seeking new energy-saving strategies to reduce energy consumption and improve energy efficiency.[3−10] Electrochromic materials have the characteristics of low consumption, high efficiency, environmental friendliness, and intelligence.[11−13] Smart windows made of electrochromic materials can adjust and control optical transmittance and heat radiation, making full use of sunlight, effectively controlling the energy exchange inside buildings, and reducing energy consumption.[14−16] In general, excellent electrochromic properties, including large optical modulation (ΔT), short coloring/bleaching response time, good charge and discharge reversibility, and long cycle stability, are required for electrochromic materials. Transition metal oxides have attracted huge attention due to their great potential.[17] Among these oxides, nickel oxide (NiO), which can be the anodic electrochromic layer in an electrochromic device (ECD), has been extensively studied because it exhibits anodic electrochromic properties and strong brown coloration.[18] It has many advantages such as good reversibility, low synthesis cost, great chemical and thermal stability, and high efficiency.[19−21] However, its electrochromic performance still cannot meet the requirement.[22]

Recently, it has been discovered that doping other elements (Li, Mg, Cu, Al, Sn, V, Co, Ag, Ta, etc.) into NiO films can effectively improve their optical modulation, response time, and cycle durability.[23,24] Zhang et al.[25] synthesized a Co-doped NiO nanoflake array by low-temperature chemical bath deposition, showing large ΔT (88.3%) and short response times (3.4 and 5.4 s). Zhao et al.[26] prepared Sn-doped NiO films by one-step magnetron sputtering for superior electrochromic performance, showing large ΔT (65.1%) and short response times (1.3 and 1.4 s). Kim et al.[27] produced a Cu-doped NiO film exhibiting an excellent areal capacitance (~14.9 mF/cm^2), superior Coulombic efficiency (~99%), and high charging/discharging cyclic stability (>10,000 cycles). Through these studies, it is not difficult to find that it is feasible to dope metal ions into NiO to improve the electrochromic

Received: December 30, 2021
Accepted: February 18, 2022
Published: February 28, 2022

ACS Publications

© 2022 The Authors. Published by American Chemical Society

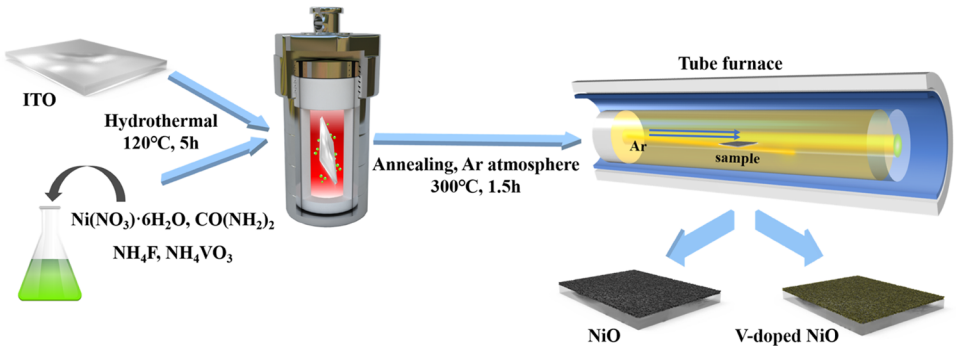

Figure 1. Preparation process of the V-doped NiO film with a patterned two-dimensional porous structure.

properties of NiO thin films.[28] In particular, among the metal ions already mentioned, the ion radius of V^{5+} (0.59 Å) is smaller than that of Ni^{2+} (0.69 Å), and V^{5+} can be easily doped into the NiO lattice. In addition, vanadium pentoxide (V_2O_5) has been used in electrochromic devices in the past few decades due to its good thermal stability, chemical stability, and electrochromic properties.[29] Therefore, we believe that NiO films can be synthesized by doping V^{5+} ions to obtain better electrochromic properties.

There are various physical and chemical methods to prepare NiO films: hydrothermal method, sonochemical method, sol–gel method, thermal decomposition method, chemical vapor deposition method, magnetron sputtering method, precipitation method, etc.[30−36] Among them, the sample synthesized by the hydrothermal synthesis method has the advantages of high purity, almost no pollution, fine particles, and controllable morphology, and it does not require expensive equipment. It has also been reported that the two-dimensional porous structure can significantly improve electrochemical performance and electrochromic performance.[37]

Therefore, we proposed to synthesize a two-dimensional porous structure of a V-doped NiO film on a glass substrate with indium tin oxide (ITO) used as an ECD anode material by the hydrothermal method. The effects of V^{5+} ion modification and different V^{5+} ion doping contents on the chemical constitution, morphology, and electrochromic properties of NiO films were studied. The electrochromic properties of the modified NiO film have been significantly improved, and to the best of our knowledge, no relevant study has been reported.

RESULTS AND DISCUSSION

Figure 1 illustrates the preparation flow chart of the two-dimensional porous structure of the V-doped NiO film. The NiO film after the hydrothermal reaction was uniformly distributed on the glass substrate, and it presented a white foggy state. The solution was light green, and the main component was $Ni_2(OH)_2CO_3{\cdot}nH_2O$. The V-doped NiO film was light yellow due to V^{5+} ions, and the solution was yellow-green. Annealing was followed to obtain the final sample.

To reveal the lattice structure of different NiO films, XRD analysis was carried out for different V-doped NiO films on the ITO substrate (Figure 2). Characteristic peaks of the ITO substrate appear in the XRD patterns of all prepared films (JCPDF#39-1058). In addition, we can observe strong crystalline peaks exhibited by NiO(111), (200), and (220) reflections,[25] indicating a highly crystalline structure. No additional characteristic peaks corresponding to vanadium

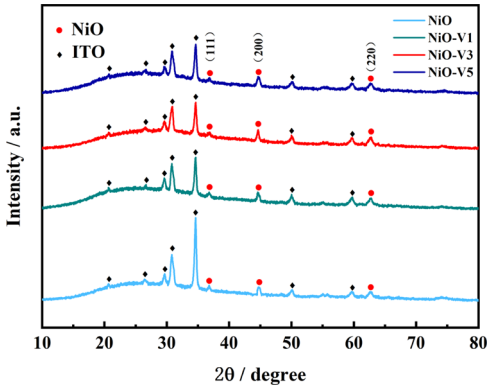

Figure 2. XRD pattern of undoped and V-doped porous nano-NiO films (NiO-V1: 1 atom % V-doped NiO; NiO-V3: 3 atom % V-doped NiO; NiO-V5: 5 atom % V-doped NiO).

and vanadium compounds or other impurities are detected, indicating that V is completely incorporated into the NiO crystal lattice or exists in the amorphous form, and the original lattice structure of the NiO film is not changed. There is no observable peak shift in the characteristic peak of NiO, demonstrating that it is a substitute doping, but as the doping amount increases, the characteristic peak of NiO gradually widens. This may be due to the smaller ion radius of V^{5+} ions, which can easily replace Ni^{2+} ions by entering the NiO lattice, making the crystal grain size smaller. Therefore, we believe that V^{5+} ions in the V-doped NiO film have completely entered the NiO lattice.

For the purpose of exploring the surface composition and chemical state of the prepared NiO thin film, the sample was characterized by X-ray photoelectron spectroscopy (XPS) analysis, as shown in Figure 3. The full spectrum of the NiO-V3 thin film is shown in Figure 3a. As shown in the illustration, we detected the characteristic peak of V 2p, which confirms the successful doping of V^{5+} ions. The fine XPS spectrum of the V 2p orbital is shown in Figure S1. The vanadium ions are mainly composed of V^{5+} ions, including a small amount of V^{4+} ions.[11,38] High-resolution spectra of Ni 2p ionized $2p_{3/2}$ spin–orbital component in NiO and NiO-V3 films are shown in Figure 3b. For NiO, Ni $2p_{3/2}$ can be deconvoluted into three peaks, corresponding to the Ni^{2+}, Ni^{3+}, and satellite peaks.[25] Among them, Ni^{2+} exists in Ni–O bonds, while Ni^{3+} exists in Ni–OH bonds.[15] Compared with the Ni $2p_{3/2}$ assigned binding energies 854.88 eV (Ni^{2+}) and 856.09 eV (Ni^{3+}) in the NiO film, those in the NiO-V3 film are 855.18 eV (Ni^{2+}) and 856.48 eV (Ni^{3+}), which are increased by 0.3 and 0.39 eV, respectively, reflecting the interaction between V^{5+}

https://doi.org/10.1021/acsomega.1c07370
ACS Omega 2022, 7, 8960−8967

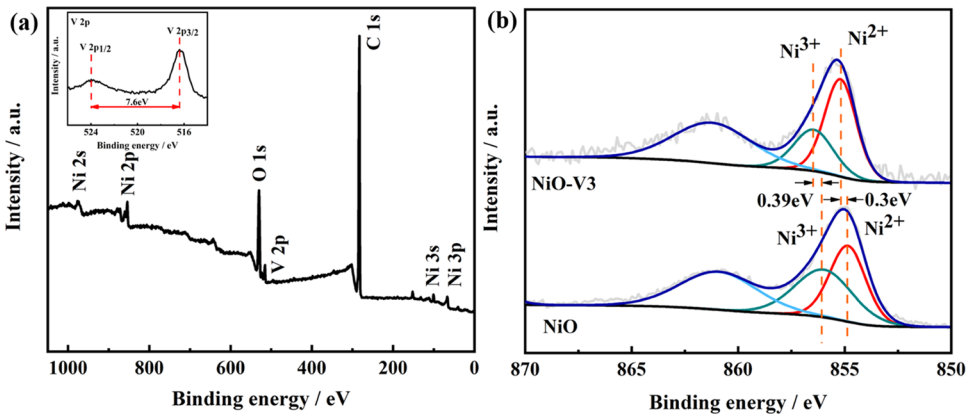

Figure 3. (a) Full spectrum of the NiO-V3 thin film, and the inset shows the V 2p spectrum. (b) Ni $2p_{3/2}$ XPS spectrum of the NiO film and the NiO-V3 thin film.

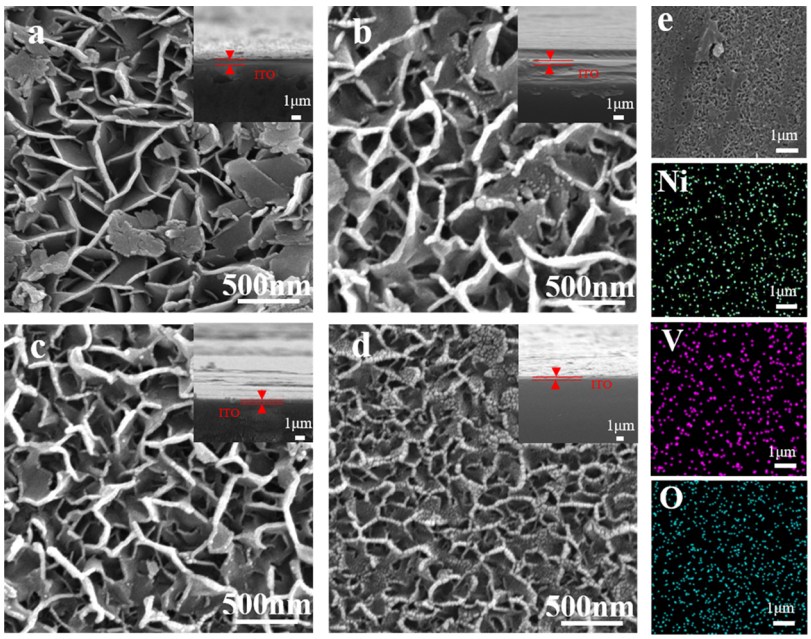

Figure 4. SEM images of NiO films with different V doping contents: (a) undoped NiO film, (b) NiO-V1, (c) NiO-V3, and (d) NiO-V5. (e) SEM image of NiO-V3 and its corresponding EDS elemental mappings.

ions and NiO. This further confirms the successful doping of V^{5+} ions. Otherwise, compared with the undoped NiO (Ni^{2+}/Ni^{3+} = 51.39/48.61%) film, the relative content of Ni^{2+} in the NiO-V3 (Ni^{2+}/Ni^{3+} = 63.02/36.98%) film increases, while the relative content of Ni^{3+} decreases. According to previous studies,[25,39] this is because V^{5+} ions replace Ni^{3+} ions after V doping, which increases the hole concentration. This also reduces the charge transfer resistance, enhances the conductivity of the film, and helps to improve its electrochromic performance.

To explore the influence of different V doping contents on the surface morphology of the NiO film, we performed scanning electron microscopy−energy-dispersive spectroscopy (SEM−EDS) characterization on the surface and cross profile of the NiO film and the V-doped NiO film, as shown in Figure 4. From the SEM image and the corresponding EDS mappings of the NiO-V3 film shown in Figure 4e, it can be proved that V^{5+} ions were successfully doped into NiO films. The electrochromic properties of the film are significantly affected by the surface microtopography since the electrochemical reaction first occurs on the surface of films. It can be seen from the SEM images that the two-dimensional porous structure of the NiO film was successfully prepared, and all of the films were uniform in appearance and connected to each other in the shape of a porous neck and provided many capillary passages for ion intercalation and deintercalation. We found that, compared to the relatively large nanoflake of the NiO film shown in Figures 4a and S2a, with the addition of V^{5+} ions and the increase in its content, the pore size of the nanoflake shown in Figures 4b−d and S2b−d gradually decreases, and the grain size also gradually decreases, resulting in many small pores being formed. It shows that V^{5+} ions can further refine the grain size of the NiO surface, which is also reported by a previous study.[26] It can increase the specific surface area of the film surface, provide more active sites, improve the reaction activity, increase the ion storage capacity, and thus improve the electrochromic properties of the NiO film. In addition, comparing the microstructure of NiO films with different doping contents, it can be found that due to the small ion radius of V^{5+} ions, it can be attached to the nanowall to modify

https://doi.org/10.1021/acsomega.1c07370
ACS Omega 2022, 7, 8960−8967

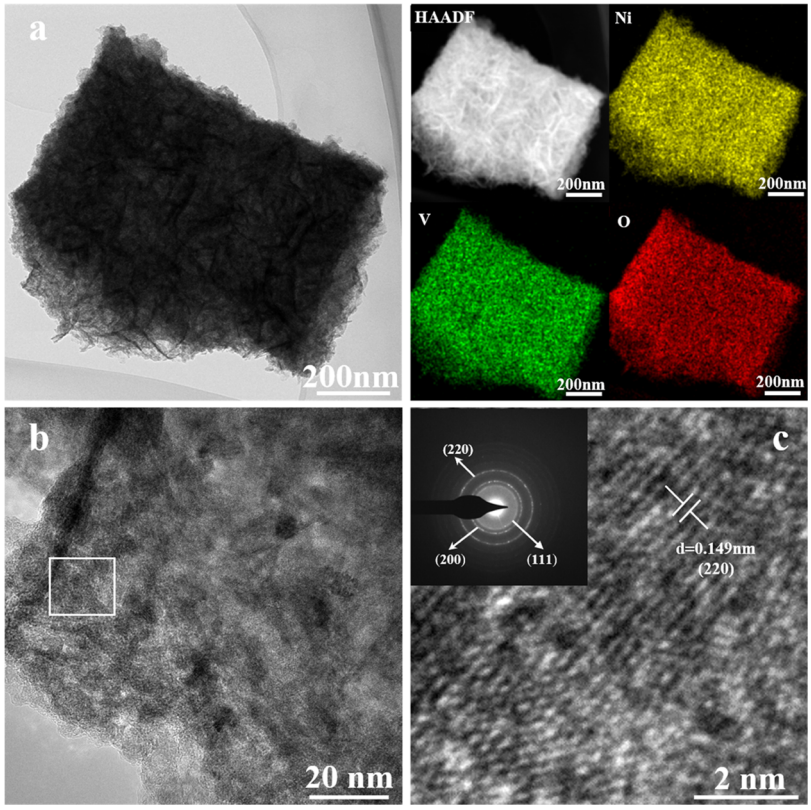

Figure 5. (a–c) TEM images and the corresponding SAED patterns of NiO-V3, and HAADF images and elemental mappings corresponding to (c).

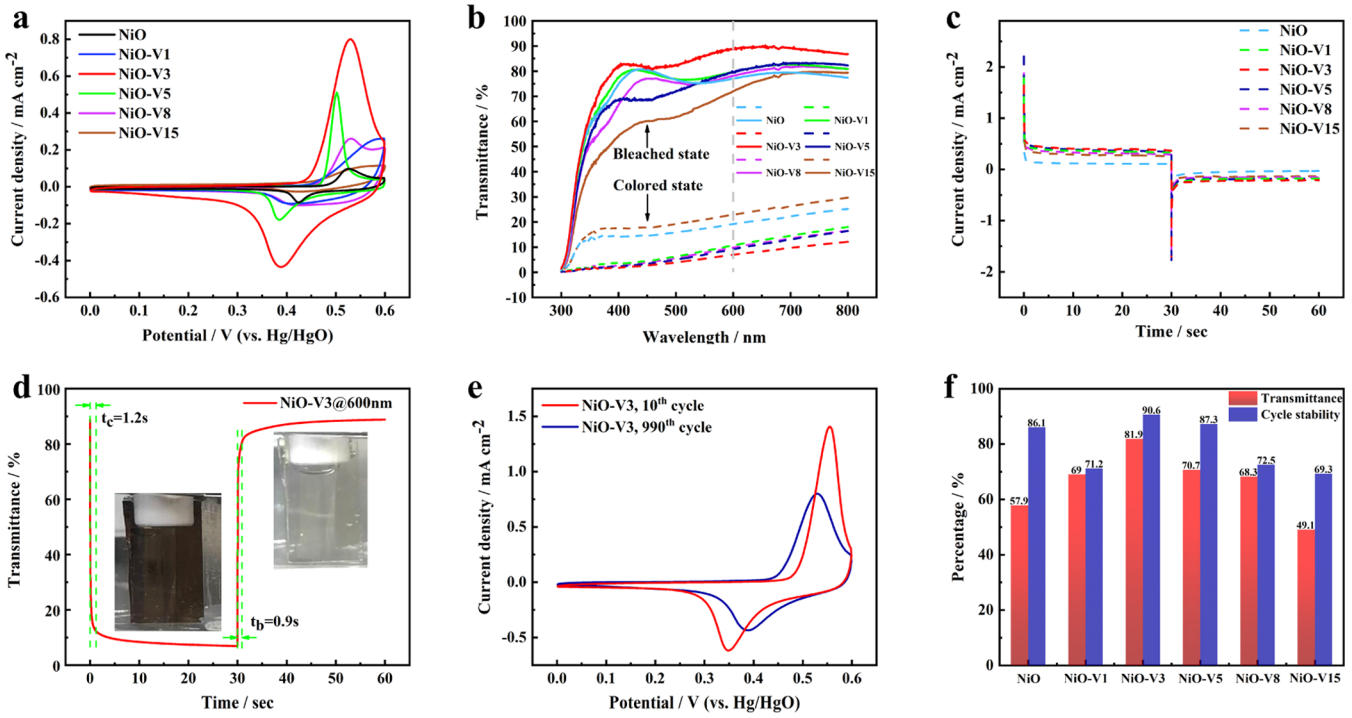

Figure 6. (a) Tenth CV curves of NiO films with different doping contents; (b) ΔT curves of NiO films with different doping contents in the state of coloring and bleaching; (c) CA curves of NiO films with different doping contents; (d) in situ transmittance of NiO-V3 at 600 nm (the illustration shows the corresponding colored and bleached photographs of NiO-V3); (e) CV curves of the 10th and 990th circles of the NiO-V3 film measured at a scanning rate of 50 mV/s under a potential range of 0–0.6 V; and (f) comparison of the ΔT and cycle stability of NiO thin films with different doping contents.

https://doi.org/10.1021/acsomega.1c07370
ACS Omega 2022, 7, 8960–8967

the surface morphology of the NiO film, thereby increasing the specific surface area of the NiO film surface. However, as the amount of doping gradually increases, as shown in Figures 4d and S2d, a large number of V^{5+} ions adhere to the walls and edges, thereby hindering charge transfer on the surface of the film. Therefore, we believe that the NiO film doped with an appropriate amount of V has the best electrochromic performance.

To further explore the morphological features and microstructure of the V-doped NiO film, high-resolution transmission electron microscopy (HRTEM) and selected area electron diffraction (SAED) technologies were used to characterize the samples. The HRTEM images shown in Figure 5a−c reveal the detailed microstructure of the NiO-V3 film. The NiO-V3 film shows a porous interconnected and well-crystallized structure and clear lattice fringes. The lattice fringe spacing is 0.149 nm, corresponding to NiO(220). Meanwhile, the SAED pattern of NiO-V3 shows the (111), (200), and (220) diffraction rings of NiO (inset of Figure 5c), indicating that the NiO film is polycrystalline, and these rings correspond to each crystal face of NiO. In addition, the distribution of Ni, V, and O in the NiO-V3 film was studied through EDS mapping. Ni, V, and O are uniformly distributed on the NiO-V3 film, indicating that V^{5+} ions are successfully doped into the NiO-V3 film. Combining the front XRD, XPS, and SEM results, it can be recognized that V has been completely incorporated into the NiO matrix and that part of the Ni^{2+} ions have been replaced by V^{5+} ions.

The electrochromic properties of the NiO film are closely related to its electrochemical properties. Besides NiO films doped with 1, 3, and 5% V atomic ratios, we also tested the electrochromic properties of NiO films with higher V atomic ratios (8 and 15%). We found that the electrochromic performance enhancement of NiO films with high V doping ratios is not ideal, as shown in Figures 6, S3, and S4 and Table 1. Therefore, the following results are mainly discussed around

Table 1. Comparison of the Electrochromic Properties of NiO Films with Different Doping Contents

	optical modulation at 600 nm			response time	
sample	T_b (%)	T_c (%)	ΔT (%)	t_b (s)	t_c (s)
NiO	77	19.1	57.9	3.4	4.1
NiO-V1	79.7	10.7	69	1.3	2.4
NiO-V3	88.8	6.9	81.9	0.9	1.2
NiO-V5	79.8	9.1	70.7	2.2	2.6
NiO-V8	78.1	9.8	68.3	2.7	3.3
NiO-V15	72	22.9	49.1	3.6	4

1, 3, and 5 atom % V-doped NiO films. We carried out cyclic voltammetry (CV) to evaluate the electrochemical performance of NiO in a potential range of 0−0.6 V at a scanning rate of 20 mV/s. As shown in Figure 6a, we compared the CV curves of NiO films with different doping contents in a 1 M KOH solution. All films show only one pair of redox peaks obviously, corresponding to the insertion and extraction of the OH^- ions. During the anode scan, Ni^{2+} is oxidized to Ni^{3+} and the color of the NiO film changes to brown. In contrast, when Ni^{3+} are reduced to Ni^{2+}, the film turns from brown to transparent, corresponding to the insertion and extraction of OH^-. This process can be illustrated by the following reaction.

$$NiO + OH^- \leftrightarrow NiOOH + e^- \quad (1)$$

or

$$NiO + H_2O \leftrightarrow NiOOH + H^+ + e^- \quad (2)$$

We can see that with increasing V doping contents, the NiO film has a higher peak current and larger integration area, indicating that it has better conductivity, ion/electron transfer ability, and charge storage ability while still having good redox reversibility and weak polarization. This shows that V doping can improve electrode utilization and optimize reaction kinetics. However, when the V doping amount increases to 5%, the redox peak current and the integral area are reduced. According to Figures 4d and S2d, excessive V doping may cause the crystal grains to be excessively refined and hinder the electrolyte transfer. At the same time, part V^{5+} ions cannot enter the NiO lattice structure and form impurities outside, which affects the specific surface area and reduces the ion transmission speed. No obvious redox peak corresponding to V was detected in the potential range, indicating that the V ion content was too low to participate in the chemical reactions. The above findings indicate that for the OH^- insertion reaction, the optimal V doping contents in the NiO film is 3 atom %.

ΔT is a very important indicator for evaluating electrochromic performance, and ΔT measurement helps to analyze the stability and reversibility of NiO films. We placed the film electrode in a 1 M KOH solution for 10 cycles of the CV test and then measured the optical transmittance of the film from the colored state and the bleached state of 300−800 nm. As shown in Figure 6b, we selected a wavelength of 600 nm, which is extremely sensitive to the human eye. We can see that V doping can greatly reduce the transmittance of the colored NiO film and increase the transmittance of the bleached state to increase the optical modulation range. The electrochromic properties of undoped and differently doped NiO films are shown in Table 1. It can be seen that 3 atom % V doping has the best optical modulation range, with ΔT as high as 81.9%, compared to 57.9% for undoped NiO films, for which it increases significantly. Better than previously reported NiO thin films (Azevedo et al.[17] reported 21% optical modulation of the V_2O_5 nanoparticle-doped NiO thin film). Subsequently, we further measured the response time of the film, which represents the time required to switch between colored and bleached states. As shown in Figures 6c,d and S4a−e, we used chronoamperometry (CA) to obtain the corresponding in situ transmittance, and we defined the response time as 90% of the time required for full transmittance modulation. All coloring and bleaching response times are shown in Table 1. The NiO-V3 film has the fastest coloring and bleaching times of 1.2 and 0.9 s, respectively, while the NiO film requires 4.1 and 3.4 s, respectively. In addition, compared with those previously reported by chemical bath deposition (3.4 and 5.4 s),[25] chemical precipitation (5.8 and 4.4 s), and electrodeposition (6 and 10 s),[40] the coloring and bleaching times of the NiO-V3 film are faster. The NiO-V3 film has an excellent light modulation range and extremely fast response times due to the two-dimensional porous nanostructure of refined grains, larger specific surface area and electrochemically active area, lower ion transfer resistance, and better conductivity and diffusion kinetics after V doping to contribute synergistically, which enhances the electrochromic properties of the NiO film. So we believe that a proper amount of V doping can improve the electrochromic performance of the NiO film.

https://doi.org/10.1021/acsomega.1c07370
ACS Omega 2022, 7, 8960−8967

Since electrochemical stability can be used to reflect the working life of the NiO films, it is an important index that determines the commercial use of the NiO films. In this study, we used the ratio of the integrated area of the 10th and 990th CV cycles to characterize the cycle stability of the film. As shown in Figures 6e,f and S3a−e, it can be noted that the undoped NiO film has good cycle stability (86.1%), which is because the stable configuration of its two-dimensional porous nanostructure reduces internal strain and better resists the volume change caused by the electrochromic process and the accompanying oxygen evolution reaction (OER) of the NiO film. Compared with the undoped NiO film, the stability of the NiO-V3 film is improved. After 990 cycles, the stability of NiO-V3 is 90.6%, which is better than that of the NiO film. Due to the improvement of the electronic conductivity of the NiO-V3 film, the effective electrochemical utilization of the film can be improved, making the insertion and extraction of ions more rapid and reducing the damage to the film during the reaction process. Therefore, the NiO-V3 film has the best light transmittance modulation and cycle stability (Figure 6f).

CONCLUSIONS

Overall, a two-dimensional porous structure of a V-doped NiO film with excellent electrochromic properties on an ITO substrate was synthesized by a hydrothermal method. V^{5+} ions modified the NiO film, including refining the crystal grains, increasing the specific surface area of the film, and accelerating the diffusion rate of OH^- in the film. Compared with the undoped NiO film, the optimized NiO-V3 film has excellent electrochromic properties, including large transmittance modulation (81.9% at 600 nm), fast response times (1.2 and 0.9 s), and excellent cycle durability (90.6%). We believe that this work can create innovation direction in the field of intelligent energy-saving window materials with high electrochromic properties.

EXPERIMENTAL SECTION

The chemicals and solvents used in this study were of analytical grade and could be used directly without further purification. All aqueous solutions were freshly prepared from high-purity water (18 MΩ/cm resistance). Nickel nitrate hexahydrate ($Ni(NO_3)_2{\cdot}6H_2O$), urea ($CO(NH_2)_2$), ammonium fluoride (NH_4F), and ammonium metavanadate (NH_4VO_3) were all purchased from Aladdin Chemical Reagent Co., Ltd. (China).

Synthesis of the NiO Film. $Ni(NO_3)_2{\cdot}6H_2O$ (3 mmol), 15 mmol of $CO(NH_2)_2$, and 6 mmol of NH_4F were dissolved in 700 mL of deionized water and stirred at a constant speed for 5 min. After that, 70 mL of the uniformly dispersed solution was added to a stainless steel autoclave lined with 100 mL of polytetrafluoroethylene. Then, a 1 × 2 cm^{-2} cleaned ITO conductive glass was placed into it with the conductive surface facing up. Subsequently, the stainless steel autoclave was sealed and kept at 120 °C for 5 h. After the hydrothermal reaction, the ITO conductive glass was taken out after cooling the stainless steel autoclave to room temperature naturally, rinsed with deionized water, and then placed in an ultrasonic machine for 30 s. This step removed the adsorbed substances that were not grown in situ on the surface of the ITO conductive glass and made the resulting sample more uniform, and the desired two-dimensional porous structure was completely exposed for optimal results. After that, the sample was placed in a 60 °C drying oven to dry for 30 min and finally was annealed at 300 °C in an argon atmosphere for 1.5 h to obtain the final product. The chemical reactions involved are demonstrated as follows

$$H_2NCONH_2 + H_2O \rightarrow 2NH_3 + CO_2 \quad (3)$$

$$CO_2 + H_2O \rightarrow CO_3^{2-} + 2H^+ \quad (4)$$

$$NH_3{\cdot}H_2O \rightarrow NH^{4+} + OH^- \quad (5)$$

$$Ni^{2+} + xF^- \rightarrow [NiF_x]^{(x-2)-} \quad (6)$$

$$2[NiF_x]^{(x-2)-} + 2CO_3^{2-} + 2OH^- + nH_2O \rightarrow Ni_2(OH)_2CO_3{\cdot}nH_2O + 2xF^- \quad (7)$$

$$Ni_2(OH)_2CO_3{\cdot}nH_2O \rightarrow 2NiO + (1+n)H_2O + CO_2(\text{annealing process}) \quad (8)$$

Synthesis of the V-Doped NiO Film. The doping solution was prepared by adding 1, 3, 5, 8, and 15 atom % NH_4VO_3 into the above nickel solution, followed by ultrasound for 10 min to completely disperse the powders, and after stirring at a constant speed for 20 min, the solution was treated according to the above nickel solution to finally obtain a V-doped NiO film.

Characterization. To analyze the crystal structures of the films, X-ray diffraction (XRD) was conducted on a PANalytical X'Pert Powder (Panalytical B.V.). The film morphology and thickness were characterized by scanning electron microscopy (SEM) on a JEOL JSM-7800F. The microstructure and texture of the film were observed by high-resolution transmission electron microscopy (HRTEM), high-angle annular dark-field scanning transmission electron microscopy (HAADF-STEM), selected area electron diffraction (SEAD), and energy-dispersive spectroscopy (EDS) mapping on a Talos F200S. The chemical component analysis of the film was performed by X-ray photoelectron spectroscopy (XPS) on an ESCALAB250-Xi, and all of the XPS binding energies were calibrated using the contaminant carbon (C 1s) as a reference. All electrochemical measurements were measured on an electrochemical workstation (CHI660E, Shanghai Chenhua Instrument Co., Ltd. China) at room temperature. In addition, the ITO glass substrate loaded with the NiO film was used as the working electrode, a platinum sheet electrode was used as the counter electrode, a Hg/HgO electrode was used as the reference electrode, and the electrochemical test was carried out in a 1 M KOH electrolyte at 25 °C. The optical transmittance modulation change and response time of the films were studied using a Shimadzu UV−vis−NIR spectrometer on an electrochemical workstation. The CV measurements were performed at 20 mV/s in a potential range of 0−0.6 V. The CA measurements were studied at −1 and 1 V for 30 s. The cycle stability of the film was measured through 1000 CV cycle tests and the 10th and 990th cycles were taken as results to avoid errors.

ASSOCIATED CONTENT

Supporting Information

The Supporting Information is available free of charge at https://pubs.acs.org/doi/10.1021/acsomega.1c07370.

https://doi.org/10.1021/acsomega.1c07370
ACS Omega 2022, 7, 8960−8967

XPS and SEM characterization; performance analysis including cyclic stability and in situ transmittance; and comparison of the NiO film doped with different elements (PDF)

AUTHOR INFORMATION

Corresponding Author

Jie Dang − *College of Materials Science and Engineering, Chongqing University, Chongqing 400044, P. R. China;* orcid.org/0000-0003-1383-8390; Email: jiedang@cqu.edu.cn

Authors

Xuhe Zhan − *National Innovation Center of High Speed Train (Qingdao), Qingdao 266108, P. R. China*

Feiyu Gao − *College of Materials Science and Engineering, Chongqing University, Chongqing 400044, P. R. China*

Qianyu Zhuang − *National Innovation (Qingdao) High Speed Train Material Research Institute Co., Ltd., Qingdao 266109, P. R. China*

Yani Zhang − *National Innovation Center of High Speed Train (Qingdao), Qingdao 266108, P. R. China*

Complete contact information is available at: https://pubs.acs.org/10.1021/acsomega.1c07370

Author Contributions

‖X.Z. and F.G. contributed equally to this work.

Notes

The authors declare no competing financial interest.

ACKNOWLEDGMENTS

The authors acknowledge the financial support from the Qingdao Science and Technology Bureau and the Management Committee of Qingdao Rail Transit Industry Demonstration Zone.

REFERENCES

(1) Cui, B.; Hu, Z.; Liu, C.; Liu, S.; Chen, F.; Hu, S.; Zhang, J.; Zhou, W.; Deng, Y.; Qin, Z.; et al. Heterogeneous lamellar-edged Fe-Ni$(OH)_2$/Ni_3S_2 nanoarray for efficient and stable seawater oxidation. *Nano Res.* **2021**, *14*, 1149−1155.

(2) Wu, H.; Lu, Q.; Zhang, J.; Wang, J.; Han, X.; Zhao, N.; Hu, W.; Li, J.; Chen, Y.; Deng, Y. Thermal shock-activated spontaneous growing of nanosheets for overall water splitting. *Nano-Micro Lett.* **2020**, *12*, No. 162.

(3) Pan, J.; Zheng, R.; Wang, Y.; Ye, X.; Wan, Z.; Jia, C.; Weng, X.; Xie, J.; Deng, L. A high-performance electrochromic device assembled with hexagonal WO_3 and NiO/PB composite nanosheet electrodes towards energy storage smart window. *Sol. Energy Mater. Sol. Cells* **2020**, *207*, No. 110337.

(4) Wang, J.; Huo, X.; Guo, M.; Zhang, M. A review of NiO-based electrochromic-energy storage bifunctional material and integrated device. *J. Energy Storage* **2021**, No. 103597.

(5) Wang, K.; Qiu, D.; Zhang, H.; Chen, G.; Xie, W.; Tao, K.; Bao, S.; Liang, L.; Gao, J.; Cao, H. Boosting charge-transfer kinetics and cyclic stability of complementary WO_3−NiO electrochromic devices via SnO_x interfacial layer. *J. Sci.: Adv. Mater. Devices* **2021**, *6*, 494−500.

(6) Lv, Z.; Ma, W.; Wang, M.; Dang, J.; Jian, K.; Liu, D.; Huang, D. Co-constructing interfaces of multiheterostructure on MXene ($Ti_3C_2T_x$)-modified 3D self-supporting electrode for ultraefficient electrocatalytic her in alkaline media. *Adv. Funct. Mater.* **2021**, *31*, No. 2102576.

(7) Wang, M.; Ma, W.; Lv, Z.; Liu, D.; Jian, K.; Dang, J. Co-doped Ni_3N nanosheets with electron redistribution as bifunctional electrocatalysts for efficient water splitting. *J. Phys. Chem. Lett.* **2021**, *12*, 1581−1587.

(8) Lv, Z.; Ma, W.; Dang, J.; Wang, M.; Jian, K.; Liu, D.; Huang, D. Induction of Co_2P growth on a MXene (Ti_3C_2Tx)-modified self-supporting electrode for efficient overall water splitting. *J. Phys. Chem. Lett.* **2021**, *12*, 4841−4848.

(9) Lv, Z.; Wang, M.; Liu, D.; Jian, K.; Zhang, R.; Dang, J. Synergetic effect of Ni_2P and MXene enhances catalytic activity in the hydrogen evolution reaction. *Inorg. Chem.* **2021**, *60*, 1604−1611.

(10) Jian, K.; Ma, W.; Lv, Z.; Wang, M.; Lv, X.; Li, Q.; Dang, J. Tuning the electronic structure of the CoP/Ni_2P nanostructure by nitrogen doping for an efficient hydrogen evolution reaction in alkaline media. *Inorg. Chem.* **2021**, *60*, 18544−18552.

(11) Xue, J.; Xu, H.; Wang, S.; Hao, T.; Yang, Y.; Zhang, X.; Song, Y.; Li, Y.; Zhao, J. Design and synthesis of 2D rGO/NiO heterostructure composites for high-performance electrochromic energy storage. *Appl. Surf. Sci.* **2021**, *565*, No. 150512.

(12) Phan, G. T.; Pham, D. V.; Patil, R. A.; Tsai, C.; Lai, C.; Yeh, W.; Liou, Y.; Ma, Y. Fast-switching electrochromic smart windows based on NiO-nanorods counter electrode. *Sol. Energy Mater. Sol. Cells* **2021**, *231*, No. 111306.

(13) Zhang, X.; Zhang, Y.; Zhao, B.; Lu, S.; Wang, H.; Liu, J.; Yan, H. Improvement on optical modulation and stability of the NiO based electrochromic devices by nanocrystalline modified nanocomb hybrid structure. *RSC Adv.* **2015**, *5*, 101487−101493.

(14) Surca, A. K.; Dražić, G.; Mihelčič, M. Low-temperature V-oxide film for a flexible electrochromic device: Comparison of its electrochromic, IR and raman properties to those of a crystalline V_2O_5 film. *Sol. Energy Mater. Sol. Cells* **2019**, *196*, 185−199.

(15) Cai, G.; Darmawan, P.; Cui, M.; Chen, J.; Wang, X.; Eh, A. L.; Magdassi, S.; Lee, P. S. Inkjet-printed all solid-state electrochromic devices based on NiO/WO_3 nanoparticle complementary electrodes. *Nanoscale* **2016**, *8*, 348−357.

(16) Choi, D.; Son, M.; Im, T.; Ahn, S.; Lee, C. S. Microstructure control of NiO-based ion storage layer with various sized NiO particles to evaluate the electrochromic performance. *Mater. Chem. Phys.* **2020**, *249*, No. 123121.

(17) Azevedo, C. F.; Balboni, R. D. C.; Cholant, C. M.; Moura, E. A.; Lemos, R. M. J.; Pawlicka, A.; Gündel, A.; Flores, W. H.; Pereira, M.; Avellaneda, C. O. New thin films of NiO doped with V_2O_5 for electrochromic applications. *J. Phys. Chem. Solids* **2017**, *110*, 30−35.

(18) Liu, C.; Zhou, W.; Zhang, J.; Chen, Z.; Liu, S.; Zhang, Y.; Yang, J.; Xu, L.; Hu, W.; Chen, Y.; et al. Air-assisted transient synthesis of metastable nickel oxide boosting alkaline fuel oxidation reaction. *Adv. Energy Mater.* **2020**, *10*, No. 2001397.

(19) Chen, H.; Ma, H.; Xia, H.; Chen, Y.; Zhang, L. Optimization parameters of NiO films by DC magnetron sputtering and improvement of electrochromic properties by a mixed electrolyte. *Opt. Mater.* **2021**, *122*, No. 111639.

(20) Li, W.; Zhang, X.; Chen, X.; Zhao, Y.; Wang, L.; Liu, D.; Li, X.; Chen, M.; Zhao, J.; Li, Y. Preparation and performance of fast-response ITO/Li-NiO/Li-WO_3/ITO all-solid-state electrochromic devices by evaporation method. *Mater. Lett.* **2020**, *265*, No. 127464.

(21) Ren, Y.; Zhou, X.; Zhang, H.; Lei, L.; Zhao, G. Preparation of a porous NiO array-patterned film and its enhanced electrochromic performance. *J. Mater. Chem. C* **2018**, *6*, 4952−4958.

(22) Kim, K.; Jeong, S.-J.; Koo, B.-R.; Ahn, H.-J. Surface amending effect of N-doped carbon-embedded NiO films for multirole electrochromic energy-storage devices. *Appl. Surf. Sci.* **2021**, *537*, No. 147902.

(23) Sahu, D. R.; Lee, Y.-H.; Wu, T.-J.; Wang, S.-C.; Huang, J. Synthesis and electrochromic property improvement of NiO films for device applications. *Thin Solid Films* **2020**, *707*, No. 138097.

(24) Wang, M.; He, Y.; Da Rocha, M.; Rougier, A.; Diao, X. Temperature dependence of the electrochromic properties of complementary NiO//WO_3 based devices. *Sol. Energy Mater. Sol. Cells* **2021**, *230*, No. 111239.

https://doi.org/10.1021/acsomega.1c07370
ACS Omega 2022, 7, 8960−8967

(25) Zhang, J.-H.; Cai, G.-F.; Zhou, D.; Tang, H.; Wang, X.-L.; Gu, C.-D.; Tu, J.-P. Co-doped NiO nanoflake array films with enhanced electrochromic properties. *J. Mater. Chem. C* **2014**, *2*, 7013−7021.
(26) Zhao, Y.; Zhang, X.; Chen, X.; Li, W.; Wang, L.; Li, Z.; Zhao, J.; Endres, F.; Li, Y. Preparation of Sn-NiO films and all-solid-state devices with enhanced electrochromic properties by magnetron sputtering method. *Electrochim. Acta* **2021**, *367*, No. 137457.
(27) Kim, S. Y.; Yun, T. Y.; Yu, K. S.; Moon, H. C. Reliable, High-performance electrochromic supercapacitors based on metal-doped nickel oxide. *ACS Appl. Mater. Interfaces* **2020**, *12*, 51978−51986.
(28) Xue, J.; Li, W.; Song, Y.; Li, Y.; Zhao, J. Visualization electrochromic-supercapacitor device based on porous Co doped NiO films. *J. Alloys Compd.* **2021**, *857*, No. 158087.
(29) Dalavi, D. S.; Bhosale, A. K.; Desai, R. S.; Patil, P. S. Energy efficient electrochromic smart windows based on highly stable CeO_2-V_2O_5 optically passive counter electrode. *Mater. Today: Proc.* **2021**, *43*, 2702−2706.
(30) Yu, Y.; Zeng, W.; Xu, M.; Peng, X. Hydrothermal synthesis of WO_3·H_2O with different nanostructures from 0D to 3D and their gas sensing properties. *Phys. E* **2016**, *79*, 127−132.
(31) Garcia, I. T. S.; Corrêa, D. S.; de Moura, D. S.; Pazinato, J. C. O.; Pereira, M. B.; Da Costa, N. B. D. Multifaceted tungsten oxide films grown by thermal evaporation. *Surf. Coat. Technol.* **2015**, *283*, 177−183.
(32) Ponzoni, A.; Comini, E.; Ferroni, M.; Sberveglieri, G. Nanostructured WO_3 deposited by modified thermal evaporation for gas-sensing applications. *Thin Solid Films* **2005**, *490*, 81−85.
(33) Marichi, R. B.; Sahu, V.; Lalwani, S.; Mishra, M.; Gupta, G.; Sharma, R. K.; Singh, G. Nickel-shell assisted growth of nickel-cobalt hydroxide nanofibres and their symmetric/asymmetric supercapacitive characteristics. *J. Power Sources* **2016**, *325*, 762−771.
(34) Hong, S. J.; Jun, H.; Borse, P. H.; Lee, J. S. Size effects of WO_3 nanocrystals for photooxidation of water in particulate suspension and photoelectrochemical film systems. *Int. J. Hydrogen Energy* **2009**, *34*, 3234−3242.
(35) Gondal, M. A.; Dastageer, M. A.; Khalil, A. Synthesis of nano-WO_3 and its catalytic activity for enhanced antimicrobial process for water purification using laser induced photo-catalysis. *Catal. Commun.* **2009**, *11*, 214−219.
(36) Gedanken, A. Using sonochemistry for the fabrication of nanomaterials. *Ultrason. Sonochem.* **2004**, *11*, 47−55.
(37) Giancaterini, L.; Emamjomeh, S. M.; De Marcellis, A.; Palange, E.; Resmini, A.; Anselmi-Tamburini, U.; Cantalini, C. The influence of thermal and visible light activation modes on the NO_2 response of WO_3 nanofibers prepared by electrospinning. *Sens. Actuators, B* **2016**, *229*, 387−395.
(38) Jeong, S.-J.; Kim, K.-H.; Ahn, H.-J. Vacancy-engineered V_2O_5-x films for ultrastable electrochromic applications. *Ceram. Int.* **2021**, *8*, 135.
(39) Mai, Y. J.; Tu, J. P.; Xia, X. H.; Gu, C. D.; Wang, X. L. Co-doped NiO nanoflake arrays toward superior anode materials for lithium ion batteries. *J. Power Sources* **2011**, *196*, 6388−6393.
(40) Yuan, Y. F.; Xia, X. H.; Wu, J. B.; Chen, Y. B.; Yang, J. L.; Guo, S. Y. Enhanced electrochromic properties of ordered porous nickel oxide thin film prepared by self-assembled colloidal crystal template-assisted electrodeposition. *Electrochim. Acta* **2011**, *56*, 1208−1212.

https://doi.org/10.1021/acsomega.1c07370
ACS Omega 2022, 7, 8960−8967